BASIC RESEARCH www.jasn.org

Disease-Causing Dysfunctions of Barttin in Bartter Syndrome Type IV

Audrey G.H. Janssen,* Ute Scholl,* Constanze Domeyer,* Doreen Nothmann,* Ariane Leinenweber,* and Christoph Fahlke*†

*Institut für Neurophysiologie, Medizinische Hochschule Hannover, and †Zentrum für Systemische Neurowissenschaften, Hannover, Germany

ABSTRACT

Bartter syndrome type IV is an inherited human condition characterized by severe renal salt wasting and sensorineural deafness. The causal gene, *BSND*, encodes barttin, an accessory subunit of chloride channels located in the kidney and inner ear. Barttin modulates the stability, cell surface localization, and function of ClC-K channels; distinct mutations cause phenotypes of varying severity. For definition of the molecular basis of this diversity, the functional consequences of six disease-causing mutations (R8L, R8W, G10S, Q32X, G47R, and E88X) on ClC-K channel properties were studied by heterologous expression in renal cell lines, electrophysiology, confocal imaging, and biochemical analysis. Three missense mutations (R8L, R8W, and G10S) eliminated the function of ClC-K/barttin channels but did not prevent the insertion of the channels into the surface membrane. Another mutant that produces a mild renal phenotype (G47R) was capable of performing all functions of wild-type barttin but bound to ClC-K channels less effectively. The nonsense mutation E88X affected epithelial sorting, leading to equal amounts of barttin inserting into the basolateral and apical membranes, contrasting with the preferential apical insertion of wild-type barttin. Last, the nonsense mutation Q32X allowed barttin to associate with ClC-K channels but prevented surface membrane insertion and channel activation. These results demonstrate that Bartter syndrome type IV can be caused by various derangements in the function of barttin, likely contributing to the diversity of observed phenotypes.

J Am Soc Nephrol 20: 145–153, 2009. doi: 10.1681/ASN.2008010102

Hypokalemic salt-losing tubulopathies (Bartter syndromes)[1] are a group of clinically and genetically distinct renal diseases, characterized by renal salt wasting, hypokalemic metabolic alkalosis, and elevated renin and aldosterone levels. Five different types of Bartter syndrome can be distinguished and correlated to different disease genes.[2,3] Among them, Bartter syndrome type IV usually exhibits a severe phenotype. Fetal polyuria causes maternal polyhydramnios,[4,5] and, postnatally, salt wasting and polyuria occur as consequences of impaired tubular reabsorption. In some patients, renal failure occurs at a young age. In addition to the renal phenotype, patients experience sensorineural deafness.[4]

The disease gene of Bartter type IV, *BSND*, encodes barttin, an accessory subunit of a subclass of ClC channels, the ClC-K channels.[6–8] Barttin mutations impair chloride absorption in various sections of the nephron as well as potassium secretion in the stria vascularis and the vestibular labyrinth.[6,9] For several disease-causing mutations, the effect on ClC-K channel functions has been previously evaluated.[6–8] In some cases though, the observed barttin dysfunction, studied using either amphibian oo-

Received January 25, 2008. Accepted June 25, 2008.

Published online ahead of print. Publication date available at www.jasn.org.

Correspondence: Dr. Christoph Fahlke, Institut für Neurophysiologie, Medizinische Hochschule Hannover, Carl-Neuberg-Strasse 1, 30625 Hannover, Germany. Phone: +49-511-532-2777; Fax: +49-511-532-2776; E-mail: fahlke.christoph@mh-hannover.de

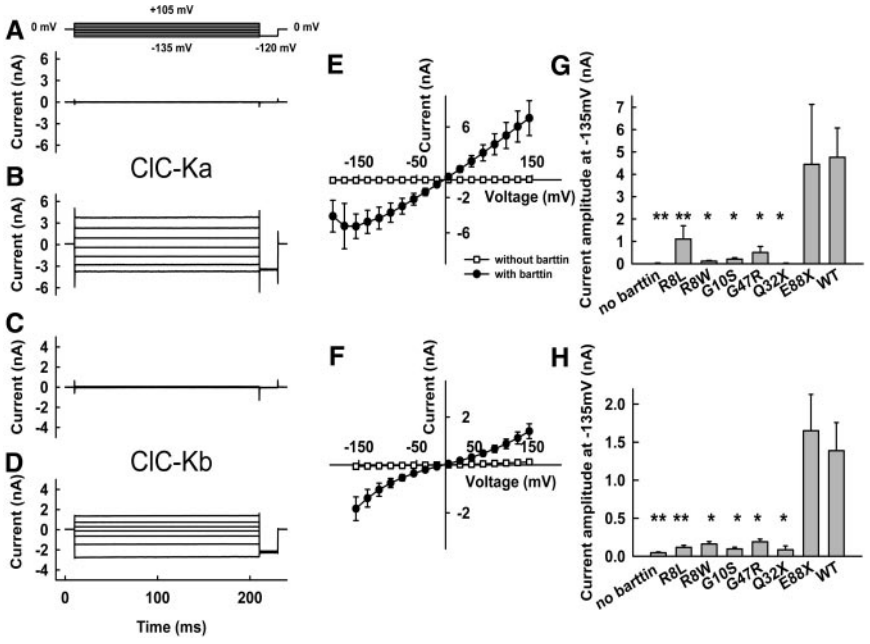

Figure 1. Disease-causing barttin mutations result in decreased amplitudes of ClC-Ka/barttin and ClC-Kb/barttin anion currents. (A through D) Representative currents from cells expressing ClC-Ka (A and B) or ClC-Kb (C and D) without (A and C) or with (B and D) barttin. (E and F) Current-voltage relationships from cells expressing ClC-Ka (E) or ClC-Kb (F) either with or without barttin ($n > 4$). (G and H) Mean isochronal current amplitudes determined at voltage steps to −135 mV from cells expressing ClC-Ka (G) or ClC-Kb (H) with various pathogenic barttin mutations ($n \geq 3$). $^{**}P < 0.01$, $^{*}P < 0.05$ *versus* WT barttin.

cytes[6,7] or rat ClC-K channels,[7,8] did not predict alterations of transepithelial transport that were sufficient to explain the disease symptoms. We therefore decided to reconsider four pathogenic missense mutations—R8L,[10] R8W,[10] G10S,[10,11] and G47R[12]—and to evaluate two novel nonsense mutations—Q32X[13] and E88X[14]—studying their effects on human ClC-Ka and ClC-Kb channels in mammalian cells. We used various experimental approaches to assess possible alterations of all known functions of barttin. For each disease-causing mutation, our analysis defines particular changes of function that correlate with the severity of disease.

RESULTS

Functional Consequences of Disease-Causing Barttin Mutations

We expressed human ClC-Ka or ClC-Kb, either with or without barttin, in tsA201 cells and measured anion currents with the patch-clamp technique (Figure 1). Whereas coexpression of barttin resulted in large anion currents for both ClC-K isoforms (Figure 1, B and D), current amplitudes were indistinguishable from the background in the absence of barttin[6,7,9,15] (Figure 1, A and C). ClC-Ka/barttin and ClC-Kb/barttin currents were independent of time and voltage (Figure 1, B and D). The current-voltage relationship of ClC-Ka/barttin was linear over a broad voltage range but decreased at very negative potentials (Figure 1E). In contrast, the voltage dependence of the ClC-Kb/barttin current amplitudes showed a slight bidirectional rectification with increasing conductances at very negative or very positive potentials (Figure 1F). With the exception of E88X, all disease-causing mutations tested caused a dramatic reduction of ClC-Ka and ClC-Kb anion currents (Figure 1, G and H).

Biochemical Characterization of ClC-K/Barttin Interaction

The absence of macroscopic current amplitudes might be due to an insufficient transcription/translation of mutant barttin, a lack of surface membrane insertion of ClC-K/barttin channels, or the loss of function of these channels. First we tested the production of mutant barttin by expressing fusion proteins of wild-type (WT) and mutant barttin covalently linked to cyan fluorescent protein (CFP). All fusion proteins tested showed good expression (Figure 2A). In SDS-PAGE, a predominant band at 63 kD was observed for WT, R8L, R8W, G10S, and G47R barttin, close to the calculated molecular weight of these fusion proteins (Figure 2A). The two nonsense mutations, E88X and Q32X, reduced the molecular weights of the fusion proteins. For all barttins tested, additional fragments with smaller molecular weights and lower intensities demonstrated proteolytic cleavage by endogenous proteases. Carboxy-terminal fragments of such sizes[15] can diffuse freely and would cause a homogeneous staining of the cell and the nucleus of transfected cells. This is not the case for full-length barttin, indicating that proteolysis does not occur in intact cells (Figures 3 and 4). For Q32X and E88X barttin, proteolysis was more pronounced (Figure 2A), indicating reduced stability of truncated barttin.

Next we resolved yellow fluorescent protein (YFP)-fusion proteins of ClC-Kb channels, expressed either alone or together with WT or mutant barttin, by reducing SDS-PAGE (Figure 2, B and C). YFP-ClC-Kb migrated as a double-fluorescence band, with molecular sizes of approximately 90 and 92 kD (calculated mass 103 kD). The higher molecular weight band disappeared upon deglycosylation with EndoH (Figure 2B), demonstrating that ClC-Kb is core-glycosylated in the absence of barttin. The differences between the apparent and calculated molecular masses are most likely

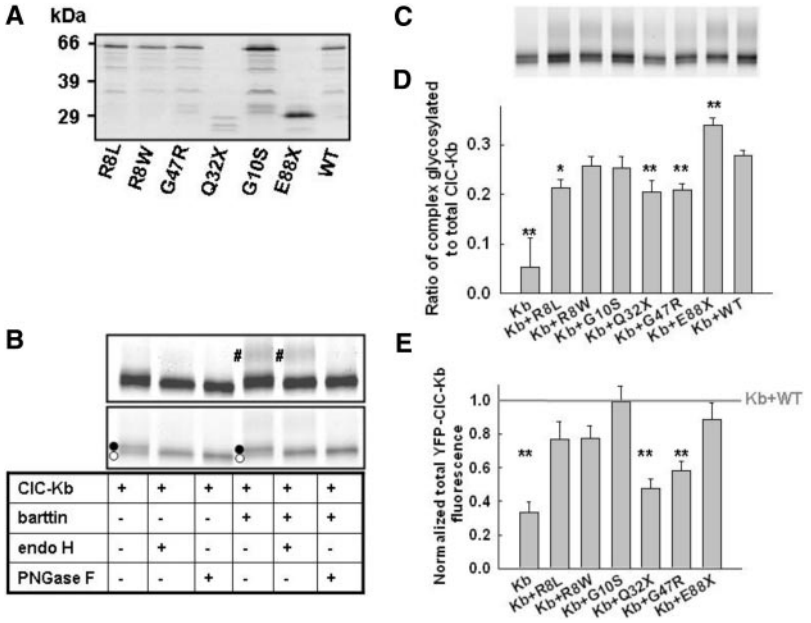

Figure 2. Biochemical analysis of barttin and ClC-Kb. (A) Fluorescence scan of an SDS-PAGE gel of CFP-tagged WT and mutant barttin proteins heterologously expressed in tsA201 cells. (B) SDS-PAGE gel (6 to 15% polyacrylamide) showing the effect of Endo-H and PNGase F on YFP-ClC-Kb glycosylation in the presence and absence of WT barttin in MDCK cells. The same gel was scanned at two different intensities to show complex glycosylation (#, top) as well as core-glycosylated (●) or not glycosylated (○) protein. (C) SDS-PAGE gel (6 to 15% polyacrylamide) of YFP-ClC-Kb either transfected alone or co-transfected with WT or mutant barttin in MDCKII cells. (D) Ratio of the intensities of complex glycosylated to total YFP-ClC-Kb fluorescence from cells coexpressing WT or mutant barttin. Data are means ± SEM from five or more experiments. (E) YFP-ClC-Kb fluorescence from cells coexpressing WT or mutant barttin from at least seven experiments. For each experiment, fluorescence was normalized to YFP-ClC-Kb fluorescence in the presence of WT barttin as indicated by the gray line. $^{**}P < 0.01$, $^{*}P < 0.05$ *versus* WT barttin.

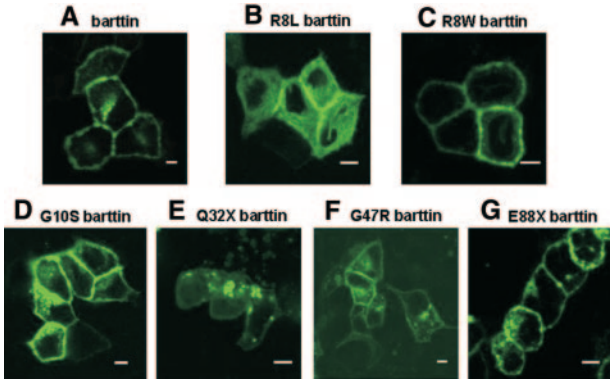

Figure 3. Subcellular distribution of WT and mutant barttin. (A through G) Fluorescence confocal images of living MDCK cells expressing WT or mutant barttin-CFP fusion proteins. Bar = 5 μm.

due to anomalous migration.[16] Coexpressing barttin resulted in an additional fluorescence band (molecular weight approximately 107 kD) that was sensitive only to PNGase F and thus represents complex-glycosylated ClC-Kb. Oligosaccharide side chains are sequentially processed from a high mannose form in the endoplasmic reticulum (ER) to the complex-glycosylated form in the Golgi apparatus, so glycosylation analysis allows quantification of the ability of barttin to promote ER exit of ClC-K channels. All mutant barttins tested yielded complex glycosylation of ClC-Kb (Figure 2, C and D). We observed comparable fractions of complex glycosylated ClC-Kb when coexpressed with WT, R8W, or G10S. Whereas R8L, Q32X, and G47R barttin impaired complex glycosylation, E88X seemed even to stimulate ER exit of ClC-K/barttin channels (Figure 2D).

WT barttin was shown to increase the number of ClC-K proteins by improving the protein stability.[8] We compared the effect of WT and mutant barttin on the number of YFP-ClC-Kb in MDCKII cells (Figure 2, C and E). Whereas Q32X and G47R significantly reduced the number of ClC-Kb channels, similar amounts of ClC-K were detected for WT, R8L, R8W, G10S, and E88X barttin (Figure 2E).

Subcellular Distribution of Mutant Barttin

We studied the subcellular distribution of barttin and ClC-K using confocal imaging of cells expressing fluorescent fusion proteins (Figures 3 and 4). Whereas WT (Figure 3A), R8W (Figure 3C), G10S (Figure 3D), and E88X (Figure 3G) were predominantly present in the plasma membrane, cells expressing R8L (Figure 3B), Q32X (Figure 3E), or, to a lesser extent, G47R (Figure 3F) barttin exhibited an increased staining of intracellular compartments.

Co-transfecting ClC-Kb with WT barttin resulted in a redistribution of chloride channels to the surface membrane[8,15] (Figure 4). Co-localization of YFP and CFP fluorescence confirmed effective binding of YFP-ClC-Kb and WT (Figure 4A) as well as G10S (Figure 4D) and E88X (Figure 4G) barttin-CFP. In contrast, Q32X abolished the redistribution of ClC-K (Figure 4E), whereas co-transfection with R8L (Figure 4B) or G47R (Figure 4F) barttin resulted in ClC-K channel insertion into the plasma membrane. In all of these cases, a variable fraction of ClC-K channels was found in intracellular compartments, and ClC-K and mutant barttins did not fully co-localize. R8W barttin exhibited less intense intracellular staining, co-localization with ClC-Kb, and effective surface membrane insertion of ClC-Kb (Figure 4C).

Surface biotinylation of transfected MDCK cells allows quantification of the effects of *BSND* mutations on membrane insertion of ClC-Kb. Surface membrane proteins were labeled with biotin, precipitated with avidin-coated beads, and analyzed by SDS-PAGE and fluorescence imaging (Figure 4H). To

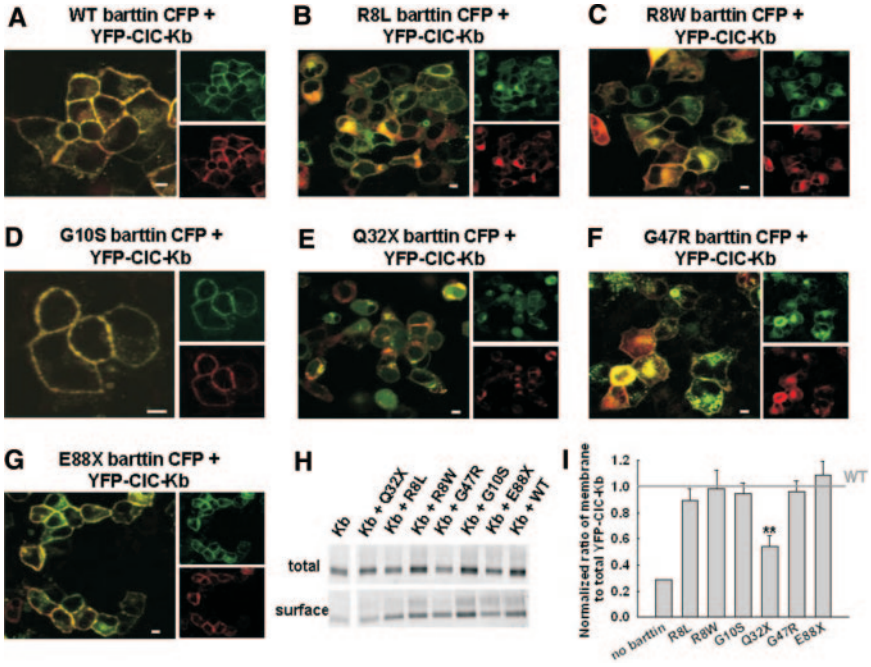

Figure 4. Effects of disease-causing barttin mutations on the localization of ClC-Kb/barttin channels in living MDCKII cells. (A through G) Representative confocal images of cells expressing YFP-ClC-Kb together with CFP tagged WT (A), R8L (B), R8W (C), G10S (D), Q32X (E), G47R (F), and E88X (G) barttin. CFP is shown in green, and YFP is shown in red. This color code results in an orange coloring of regions where both proteins overlap. Individual YFP and CFP fluorescences are added to demonstrate co-localization of WT barttin and ClC-Kb. Bar = 5 μm. (H) Fluorescence scan of an SDS-PAGE gel of YFP-ClC-Kb present in the total cleared lysate and the purified surface proteins, when expressed alone or in the presence of WT or mutant barttin. (I) Membrane surface insertion of ClC-Kb by mutant barttin was quantified by dividing the fluorescence of surface-biotinylated YFP-ClC-Kb by the fluorescence of the total cleared lysate and normalization to the ratio found in the presence of WT barttin. Data are means ± SEM from three experiments. $^{**}P < 0.01$.

account for effects of barttin on the abundance of ClC-K protein, we divided fluorescence intensities from surface proteins by the YFP fluorescence of the full lysate. These ratios were normalized to data obtained with WT barttin (Figure 4I) to determine the capability of mutant barttin to insert ClC-K channels into the surface membrane. R8L, R8W, G10S, G47R, and E88X barttin increased relative amounts of ClC-K in the surface membrane to the same extent as WT barttin. Of all tested barttin mutants, only Q32X reduced the percentage of ClC-K in the surface membrane.

The plasma membrane of epithelial cells is divided into an apical and a basolateral domain with distinct transporters and channels, making transepithelial vectorial transport possible. E88X does not affect macroscopic ClC-K currents and thus might exclusively affect epithelial sorting. We first studied epithelial sorting for WT and E88X barttin in MDCK cells grown on filters. Confocal sections of cell lines stably expressing WT or E88X barttin-CFP allowed separation of barttin in basolateral and apical membranes (Figure 5). Whereas WT barttin sorts predominantly to the basolateral membrane (Figure 5A), there is a much more pronounced apical staining of E88X barttin-CFP (Figure 5B). To quantify this alteration of epithelial sorting, we performed surface biotinylation in confluent monolayers of MDCK cells grown on filters (Figure 5, C and D). Figure 5C displays the fluorescence scan of an SDS-PAGE gel with purified membrane–inserted ClC-Kb. Figure 5D shows the relative amounts of biotinylated ClC-Kb after biotin application to the apical or the basolateral site. Whereas ClC-Kb/WT barttin preferentially inserted into the basolateral membrane, E88X resulted in equal amounts of ClC-Kb in the apical and the basolateral membranes.

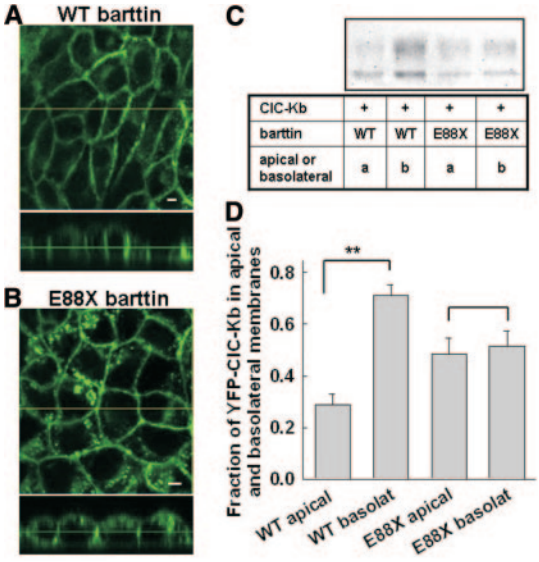

Figure 5. Epithelial sorting of ClC-Kb by WT and mutant barttin. (A and B) Confocal images of polarized MDCK cells stably expressing WT (A) or E88X (B) barttin-CFP. Cells were grown on filters and fixed before imaging. x-y projections (front view) are given in the upper part, x-z projections (side view) in the lower part. Bar = 5μm. (C) Fluorescence scan of an SDS-PAGE of YFP-ClC-Kb purified by surface biotinylation from basolateral and apical membranes of MDCK cells expressing WT or mutant barttin together with YFP-ClC-Kb. (D) Relative amounts of ClC-Kb channels in the apical and the basolateral membrane. YFP-ClC-Kb surface-biotinylated from the apical or the basolateral membrane was quantified by YFP fluorescence, adjusted for actin amounts, and then given as relative amount of the total surface fluorescence. Data are means ± SEM from five experiments. $^{**}P < 0.01$.

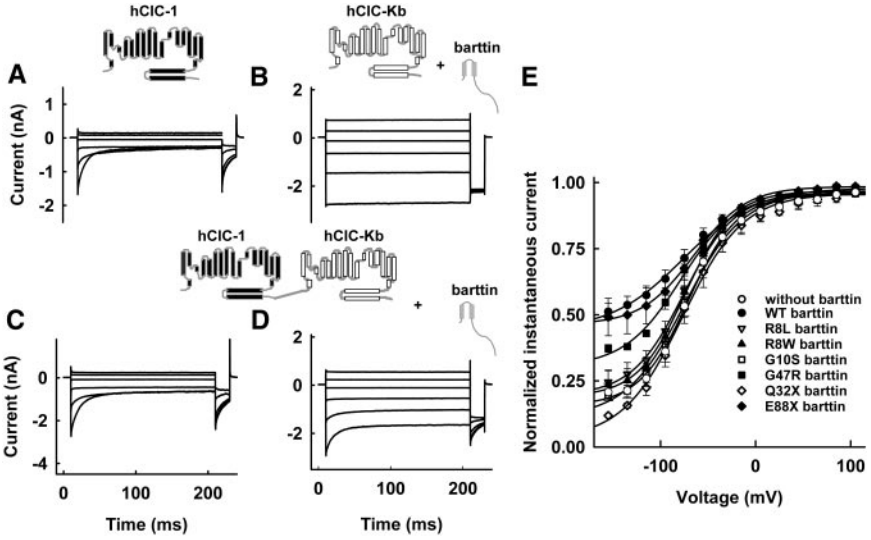

Figure 6. Pathogenic missense mutations affect the function of ClC-K/barttin channels. (A through D) Representative current recordings from cells expressing hClC-1 alone (A), ClC-Kb with barttin (B), concatameric hClC-1-ClC-Kb without barttin (C), or together with barttin (D). (E) Voltage dependence of the normalized instantaneous current amplitude from cells expressing hClC-1-ClC-Kb concatamers alone or together with WT or mutant barttin. Data are means ± SEM from between two and seven cells.

Disease-Causing Mutations Affect the Ability of Barttin to Switch ClC-Kb into an Anion-Conducting State

The results presented so far indicate that the tested missense mutations impair membrane insertion of ClC-Kb/barttin only moderately. The main effect of these mutations must therefore be a loss of barttin's ability to switch ClC-K into an anion-conducting mode.[15] We studied this function by measuring the currents conducted by an hClC-1-ClC-Kb concatamer, linking ClC-Kb covalently to the human muscle isoform hClC-1[15] (Figure 6). Because ClC channels are double barreled,[17,18] the expression of this construct results in the insertion of heterodimeric channels with one hClC-1 and one ClC-Kb protopore into the surface membrane. In the absence of barttin, only the hClC-1 protopore is functional[15] (Figure 6, A and C). Cotransfection of barttin resulted in the addition of a voltage-independent component, thus indicating conversion of ClC-Kb protopores, which are attached to ClC-1 and therefore present in the surface membrane, into an active state (Figure 6, B and D).

To quantify the relative numbers of functional ClC-1 and ClC-Kb protopores, we measured the instantaneous current amplitudes at a fixed voltage step to −120 mV, after prepulses to various voltages. If none of the ClC-Kb protopores are functional, then the voltage dependence of this current will resemble the activation curve of ClC-1.[19] An increasing number of functional ClC-Kb results in an increased voltage-independent current component. E88X barttin activated ClC-Kb protopores as effectively as WT barttin. G47R barttin exhibited an intermediate phenotype. All other naturally occurring mutations did not activate ClC-Kb (Figure 6E).

Modification of rClC-K1 Gating by Mutant Barttins

Whereas ClC-Ka or ClC-Kb require the accessory subunit to become anion conducting, rat ClC-K1 is functional without barttin, and barttin modulates only channel gating.[15] The barttin-induced changes of gating are particularly prominent for a mutant rClC-K1 channel carrying a glutamate instead of a valine at position 166.[15] Without barttin, V166E rClC-K1 channels were activated by membrane hyperpolarization (Figure 7A), whereas co-transfection of barttin inverted the voltage dependence of activation (Figure 7B). Expression of Q32X barttin did not result in changes of the time and voltage dependence of V166E rClC-K1 (Figure 7C). In contrast, all other mutant barttins tested yielded an inversion of the voltage dependence of gating (Figure 7D).

The effect on V166E rClC-K1 gating allows a quantitative description of the interaction of ClC-K and mutant barttin. Figure 7 shows representative nonstationary variance analyses from tsA201 cells coexpressing V166E rClC-K1 channels with WT or G47R barttin. Variances (σ^2) were plotted *versus* the corresponding mean current amplitude (I; Figure 7, E and F), and numbers of channels and absolute open probabilities (Figure 7G) were obtained by fitting variance-mean current plots with $\sigma^2 = iI - I^2/N$[15,19,20] from these experiments and from comparable ones on R8L, G10S, and E88X.

G47R and R8L yield increased minimum absolute open probabilities and decreased maximum open probabilities. The changes of gating in V166E rClC-K1 induced by G47R or R8L barttin are fully consistent with a fraction of channels lacking the accessory subunit, indicating impaired binding of R8L or G47R barttin. In contrast, ClC-K channels associated with G10S or E88X barttin exhibited absolute open probabilities similar to WT.

DISCUSSION

We evaluated the functional consequences of four missense and two nonsense mutations in the *BSND* gene found in patients with Bartter syndrome type IV. R8L, R8W, G10S, and Q32X abolished epithelial anion conductance by affecting barttin's ability to activate human ClC-K channels. Q32X and G47R decreased the number of ClC-K/barttin channels. E88X

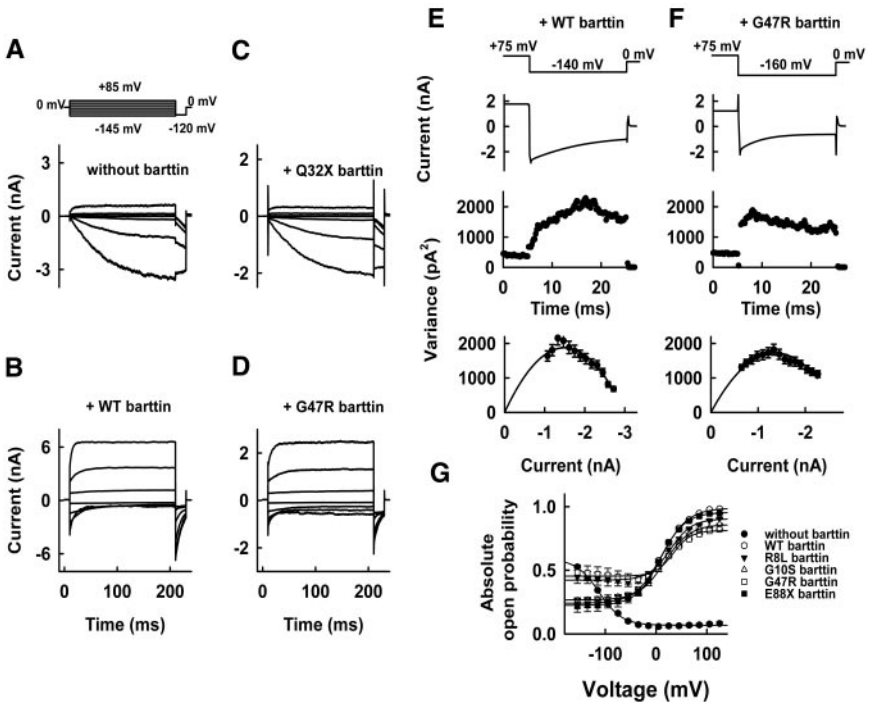

Figure 7. Modification of V166E rClC-K1 by WT or mutant barttin. (A through D) Representative current recordings from cells expressing V166E rClC-K1 channels, without barttin (A) or with WT (B), Q32X (C), or G47R (D) barttin. (E and F) Time dependences of the mean current amplitudes and variances on the given pulse protocols, and plots of variances *versus* mean current amplitudes for V166E rClC-K1 channels, with WT (E) or G47R (F) barttin. The solid lines are fits of the function $\sigma^2 = iI(t) - I(t)^2/N$. (G) Voltage dependence of the absolute open probabilities of V166E rClC-K1/mutant barttin channels. Data are means ± SEM from at least seven cells.

affected epithelial sorting, abolishing the preferential insertion of ClC-K/barttin channels into the basolateral membrane.

Q32X truncates barttin after its first putative transmembrane domain and therefore is the most pronounced change of primary sequence evaluated here. Coexpression of Q32X barttin with ClC-Ka or ClC-Kb did not result in anion currents in heterologous expression systems (Figure 1) and abolished the effect of barttin on surface membrane insertion (Figure 4).

R8L and R8W modify the subcellular distribution of barttin (Figures 3 and 4), in agreement with previous reports.[8] Nonetheless, the mutations do not prevent surface membrane insertion of ClC-Kb channels (Figure 4), so impaired trafficking alone does not explain the virtual absence of anion current. Coexpression of R8L or R8W barttin with the hClC-1-ClC-Kb concatamer resulted in heterodimeric channels with only the hClC-1 protopore active. R8L and R8W barttin are therefore not capable of switching human ClC-K channels to an active conformation. Another missense mutation, G10S, left surface membrane insertion of ClC-K channels virtually unaffected in our heterologous expression system (Figures 3 and 4)[8] and reduced the chloride conductance of epithelial cells solely by affecting barttin's ability to activate human ClC-K channels (Figure 6). The absence of currents in cells coexpressing ClC-K with G10S barttin contradicts previous results using *Xenopus* oocytes.[6] ClC-K channels are functionally different when expressed in oocytes or mammalian cells.[6,7,15] Expression in renal cell lines resembles the situation in native tissue better than amphibian oocytes, and we thus conclude that G10S abolishes plasmalemmal ClC-K/barttin currents in the human kidney.

G47R was the only missense mutation tested that did not prevent the activation of ClC-Kb/barttin channels (Figure 6); however, G47R impairs expression levels and complex glycosylation of ClC-Kb (Figure 2). All findings are fully explained by a reduced binding of G47R barttin to ClC-K. A larger number of channels lacking barttin led to retention in intracellular compartments (Figure 4), a less effective activation of ClC-Kb (Figure 6), and the observed gating alterations of rClC-K1 (Figure 7). These changes effectively downregulated the cellular chloride conductance, resulting in dramatically reduced macroscopic ClC-K/G47R currents (Figure 1). The effects of E88X on epithelial sorting (Figure 5) will impair vectorial transport in the thick ascending limb of Henle and in the stria vascularis.

All of our experiments were done in a heterologous expression system, and it is possible that native cells might differ in the expression of additional proteins that modify the functional effects of the disease-causing mutations; however, MDCK cells are an established model system to study epithelial transport and epithelial sorting, and we therefore are confident that the effects of mutant barttin on channel function and channel trafficking can be reliably studied in these cells. As in native cells,[6] ClC-Kb/barttin preferentially sorts to the basolateral membranes of MDCK cells (Figure 5). Moreover, heterologously expressed ClC-K channels functionally resemble native channels.[21] The presentation of patients with Bartter type IV shows remarkable variation, ranging from prenatal diagnosis with severe polyhydramnios and prematurity[11] to diagnosis at age 28.[22] The good correlation between the mutation-induced functional alterations observed in heterologous expression systems and the severity of the disease is a strong argument that our results predict the dysfunction of mutant barttin in native cells.

ClC-K/barttin channels are nonfunctional when barttin carries the mutations R8L, R8W, G10S, and Q32X. This fully

explains deafness and renal salt-wasting in affected patients. G47R was reported in patients with an adult onset of renal symptoms, and the less pronounced renal phenotype nicely correlates to the preserved function of G47R barttin. The distribution of ClC-K/E88X barttin between the apical and the basolateral membrane is dramatically changed compared with ClC-K/WT barttin. Such an alteration will reduce transepithelial transport and predicts the hearing impairment and renal symptoms.

Mutations leading to a loss of start codon seem to be associated with a severe course and early deterioration of renal function.[5,10] In contrast, renal function was preserved in all patients carrying barttin mutations that do not prevent insertion into the surface membrane (*i.e.*, homozygous patients with R8L [Dr. Georges Deschênes, Hôpital Robert-Debré, Paris, France; personal communication, January 29, 2008]), G10S,[11] G47R,[12,22,23] or E88X mutations.[14] Clinical data for the R8W mutation were not available. Clinical evaluation of the Q32X mutant was limited to the compound heterozygous state with another G47R allele[13]; however, compared with homozygous G47R patients, this case was distinct for end-stage renal failure at age 15. We cannot exclude that there are other functions of barttin that are not well represented in our assays, such as interaction with other membrane proteins potentially involved in the preservation of renal function; however, it occurs to us that the residual insertion of barttin into the plasma membrane we observed for most of the mutants studied—even with severely impaired ClC-K function—might protect from renal failure, potentially by an effect on currently unknown proteins and similar to the scaffolding function observed for ClC-K channels. Our observation is limited, however, to the small number of patients reported and a lack of understanding of the molecular mechanisms. Certainly, further studies are needed to assess a potential role of barttin apart from its effect on ClC channels.

CONCISE METHODS

Mutagenesis and Channel Expression

tsA201 and MDCKII cells were transfected with plasmid DNA encoding ClC-Ka,[24] ClC-Kb,[24] mutant rClC-K1[25] (pSVL-ClC-K or pRc-CMV-ClC-K), human barttin[10] (pcDNA3.1-barttin), or pcDNA3.1-GFP-EAAT3[26] using a calcium phosphate precipitation method[27] or Lipofectamine 2000 (Invitrogen, Carlsbad, CA). Mutant barttins were constructed by PCR-based strategies as CFP fusion proteins. For all constructs, PCR-amplified sequences were verified by direct sequencing, and two independent mutant clones were used for expression studies. For identification of transfected cells, barttin was co-transfected as CFP-fusion protein. Alternatively, a bicistronic vector containing the coding region of the respective ClC-K channel and of the CD8 antigen (pRcCMV or pSVL-ClC-K-IRES-CD8) was used, or a plasmid encoding the CD8 antigen was co-transfected. Cells were incubated 5 min before use together with polystyrene microbeads precoated with anti-CD8 antibodies (Dynabeads M-450 CD 8; Dynal, Great Neck, NY),[28] and only cells decorated with microbeads were used for electrophysiologic recordings. CFP or YFP fusion proteins of ClC-K channels and barttin were constructed as described previously.[29] The percentage of cells that express only ClC-K but not barttin in co-transfection experiments was obtained from confocal images of cells coexpressing YFP-ClC-Kb and Barttin-CFP. Approximately 50% of all cells expressed both proteins, whereas approximately 2% expressed only ClC-K. No differences in these numbers could be observed between WT and mutant barttin. Stable MDCK cell lines expressing WT or E88X barttin-CFP were generated by selection with geneticin[30] (Figure 5).

Electrophysiology

Whole-cell patch-clamp recordings were performed using an EPC10 amplifier (HEKA Electronics, Lambrecht, Germany). Pipettes were pulled from borosilicate glass (Harvard Apparatus, Holliston, MA) and had resistances of 1.0 to 2.2 MΩ. The series resistance was compensated 60 to 80% by an analog procedure, so the calculated voltage error as a result of access resistance was always <2 mV. The extracellular solution contained 140 mM NaCl, 4 mM KCl, 2 mM $CaCl_2$, 1 mM $MgCl_2$, and 5 mM HEPES, whereas the intracellular solution contained 120 mM NaCl, 2 mM $MgCl_2$, 5 mM EGTA, and 10 mM HEPES. Both solutions were adjusted to pH 7.4 with NaOH.

Data were analyzed by a combination of PulseTools (HEKA Electronics, Lambrecht, Germany) and SigmaPlot (Jandel Scientific, San Rafael, CA). For determination of the absolute open probabilities of V166E rClC-K1, nonstationary noise analysis was performed as described previously.[15,19]

Biochemical Analysis

MDCKII cells were lysed by incubation in 1% Triton X-100, in the presence of protease inhibitors (Sigma-Aldrich, Hamburg, Germany). Cleared lysates were denatured for 15 min at room temperature in SDS sample buffer containing 100 mM dithiothreitol and electrophoresed in parallel with fluorescence mass markers (Dual Color; Bio-Rad, München, Germany) on 6 to 15% SDS polyacrylamide gradient gels. YFP-tagged proteins were visualized by scanning the wet PAGE gels with a fluorescence scanner (Typhoon; GE Healthcare, München, Germany). Individual bands were quantified with the ImageQuant software (GE Healthcare, Freiburg, Germany). For investigation of the glycosylation state of the proteins, samples were treated for 4 h with either endoglycosidase H (EndoH) or N-glycosidase F (PNGase F; New England Biolabs, Beverly, MA) in the presence of reducing SDS sample buffer and 1% (wt/vol) NP-40 to counteract SDS inactivation of PNGase F.

Cell surface expression of barttin and ClC-K channels was assayed with a modification of cell surface biotinylation methods described previously.[30,31] MDCK cells, grown either nonconfluently on cell culture plates (Figure 4) or confluently on filters (Figure 5), were transfected with ClC-Kb alone or together with barttin fluorescence protein-fusion proteins. One day after transfection, the cells were incubated with 1.5 mg of biotin (sulfo-NHS-LC-biotin or sulfo-NHS-SS-biotin; Pierce, Rockford, IL) in PBS or triethanolamine buffer for 1 to 2 h. In experiments using filters, the side not incubated with biotin was incubated with biotinylation buffer only. The reaction was

quenched by repeated washing with quenching buffer (100 mM glycine in PBS). After washing with PBS, the cells were scraped in lysis buffer (150 mM NaCl, 1% Triton X-100, and 5 mM EDTA with 50 mM Tris or 10 mM HEPES) and transferred to a tube. After 1 h on ice, they were centrifuged at 14,000 $\times$ *g* for 10 min at 4°C, and the cell lysate was collected. Cell lysates were incubated with Ultralink immobilized NeutrAvidin beads (Pierce) for 2 h. After washing with either lysis buffer or high-salt wash buffer, the proteins on the beads were released by incubation with SDS loading buffer containing 200 mM dithiothreitol and 4.1% SDS. The proteins were separated on 6 to 15% polyacrylamide gradient gels and visualized by scanning the wet SDS-PAGE gels with a fluorescence scanner (Typhoon, GE Healthcare). The gels were blotted onto polyvinylidene (Bio-Rad) and developed with rabbit anti-actin (Sigma-Aldrich, Hamburg, Germany) and anti-rabbit Cy5 (GE Healthcare, Freiburg, Germany). Results were used only from experiments in which no actin was detected in purified membrane fractions. The amount of actin present in the cleared lysate was used to adjust the obtained data to the number of lysed cells. For biotinylation experiments on polarized MDCK cells, apical and basolateral fluorescences were added, and the amount of apical/basolateral channels are given as fraction of the total surface channels. An apical protein, GFP-EAAT3,[30] was used as control protein; 89 $\pm$ 3.7% (n = 4) of GFP-EAAT3 inserted into the apical membrane.

Confocal Microscopy

Transiently or stably transfected MDCKII cells were either grown on special confocal tissue culture treated dishes (80136; Ibidi, Martinsried, Germany) or on poly-L-lysine–treated glass coverslips and scanned as living cells 1 to 3 d after transfection or grown on filters. These filters were fixed in 4% paraformaldehyde before placement in buffer in the previously mentioned dishes. Confocal imaging was carried out with a Fluoview 1000 (Olympus, Hamburg, Germany) or a Zeiss LSM 510 confocal microscope (Carl Zeiss, Köln, Germany).

Statistical Analysis

Data are shown as means $\pm$ SEM; n reflects number of cells. Unpaired t test was used to compare mean values, and $P < 0.05$ or $P < 0.01$ was used to indicate statistical significance.

ACKNOWLEDGMENTS

These studies were supported by the Deutsche Forschungsgemeinschaft.

Parts of this study were reported as abstract (*Acta Physiol* 189: O06-2, 2007; and *Acta Physiol* 192: OM216, 2008).

This article is dedicated to the memory of Dr. Steven C. Hebert (1946 to 2008). We thank Dr. Simon Hebeisen and Dr. Patricia Hidalgo for helpful discussions; Birgit Begemann for excellent technical support; Dr. Symeon Papadopoulos, Dr. Rudolf Bauerfeind, and Dr. Alexander Polster for help with the confocal microscopy; Dr. Al George, Dr. Matthias Hediger, and Dr. Shinichi Uchida for providing the expression constructs for hClC-Ka, hClC-Kb, rClC-K1, hEAAT3, and barttin; and Dr. Michael Hanna (Medical Manuscript Service, New York, NY) for proofreading the manuscript.

DISCLOSURES

None.

REFERENCES

1. Bartter FC, Pronove P, Gill JR Jr, MacCardle RC: Hyperplasia of the juxtaglomerular complex with hyperaldosteronism and hypokalemic alkalosis: A new syndrome. *Am J Med* 33: 811–828, 1962
2. Simon DB, Lifton RP: Ion transporter mutations in Gitelman's and Bartter's syndromes. *Curr Opin Nephrol Hypertens* 7: 43–47, 1998
3. Hebert SC: Bartter syndrome. *Curr Opin Nephrol Hypertens* 12: 527–532, 2003
4. Landau D, Shalev H, Ohaly M, Carmi R: Infantile variant of Bartter syndrome and sensorineural deafness: A new autosomal recessive disorder. *Am J Med Genet* 59: 454–459, 1995
5. Jeck N, Reinalter SC, Henne T, Marg W, Mallmann R, Pasel K, Vollmer M, Klaus G, Leonhardt A, Seyberth HW, Konrad M: Hypokalemic salt-losing tubulopathy with chronic renal failure and sensorineural deafness. *Pediatrics* 108: E5, 2001
6. Estevez R, Boettger T, Stein V, Birkenhäger R, Otto E, Hildebrandt F, Jentsch TJ: Barttin is a Cl^- channel beta-subunit crucial for renal Cl^- reabsorption and inner ear K^+ secretion. *Nature* 414: 558–561, 2001
7. Waldegger S, Jeck N, Barth P, Peters M, Vitzthum H, Wolf K, Kurtz A, Konrad M, Seyberth HW: Barttin increases surface expression and changes current properties of ClC-K channels. *Pflugers Arch* 444: 411–418, 2002
8. Hayama A, Rai T, Sasaki S, Uchida S: Molecular mechanisms of Bartter syndrome caused by mutations in the BSND gene. *Histochem Cell Biol* 119: 485–493, 2003
9. Uchida S, Sasaki S: Function of chloride channels in the kidney. *Annu Rev Physiol* 67: 759–778, 2005
10. Birkenhäger R, Otto E, Schurmann MJ, Vollmer M, Ruf EM, Maier-Lutz I, Beekmann F, Fekete A, Omran H, Feldmann D, Milford DV, Jeck N, Konrad M, Landau D, Knoers NV, Antignac C, Sudbrak R, Kispert A, Hildebrandt F: Mutation of BSND causes Bartter syndrome with sensorineural deafness and kidney failure. *Nat Genet* 29: 310–314, 2001
11. Shalev H, Ohali M, Kachko L, Landau D: The neonatal variant of Bartter syndrome and deafness: Preservation of renal function. *Pediatrics* 112: 628–633, 2003
12. Garcia-Nieto V, Flores C, Luis-Yanes MI, Gallego E, Villar J, Claverie-Martin F: Mutation G47R in the BSND gene causes Bartter syndrome with deafness in two Spanish families. *Pediatr Nephrol* 21: 643–648, 2006
13. Kitanaka S, Sato U, Maruyama K, Igarashi T: A compound heterozygous mutation in the BSND gene detected in Bartter syndrome type IV. *Pediatr Nephrol* 21: 190–193, 2006
14. Ozlu F, Yapicioglu H, Satar M, Narli N, Ozcan K, Buyukcelik M, Konrad M, Demirhan O: Barttin mutations in antenatal Bartter syndrome with sensorineural deafness. *Pediatr Nephrol* 21: 1056–1057, 2006
15. Scholl U, Hebeisen S, Janssen AG, Muller-Newen G, Alekov A, Fahlke Ch: Barttin modulates trafficking and function of ClC-K channels. *Proc Natl Acad Sci U S A* 103: 11411–11416, 2006
16. Gendreau S, Voswinkel S, Torres-Salazar D, Lang N, Heidtmann H, Detro-Dassen S, Schmalzing G, Hidalgo P, Fahlke Ch: A trimeric quaternary structure is conserved in bacterial and human glutamate transporters. *J Biol Chem* 279:39505–39512, 2004
17. Miller C: Open-state substructure of single chloride channels from *Torpedo* electroplax. *Philos Trans R Soc Lond B Biol Sci* 299: 401–411, 1982
18. Dutzler R, Campbell ED, Cadene M, Chait MB, MacKinnon R: X-ray structure of a ClC chloride channel at 3.0 A reveals the molecular basis of anion selectivity. *Nature* 415: 287–294, 2002
19. Hebeisen S, Heidtmann H, Cosmelli D, Gonzalez C, Poser B, Latorre R, Alvarez O, Fahlke Ch: Anion permeation in human ClC-4 channels. *Biophys J* 84: 2306–2318, 2003

20. Sigworth FJ: The variance of sodium current fluctuations at the node of Ranvier. *J Physiol* 307: 97–129, 1980
21. Uchida S, Sasaki S, Nitta K, Uchida K, Horita S, Nihei H, Marumo F: Localization and functional characterization of rat kidney-specific chloride channel, ClC-K1. *J Clin Invest* 95: 104–113, 1995
22. Miyamura N, Matsumoto K, Taguchi T, Tokunaga H, Nishikawa T, Nishida K, Toyonaga T, Sakakida M, Araki E: Atypical Bartter syndrome with sensorineural deafness with G47R mutation of the beta-subunit for ClC-Ka and ClC-Kb chloride channels, barttin. *J Clin Endocrinol Metab* 88: 781–786, 2003
23. Brum S, Rueff J, Santos JR, Calado J: Unusual adult-onset manifestation of an attenuated Bartter's syndrome type IV renal phenotype caused by a mutation in BSND. *Nephrol Dial Transplant* 22: 288–289, 2007
24. Kieferle S, Fong P, Bens M, Vandewalle A, Jentsch TJ: Two highly homologous members of the ClC chloride channel family in both rat and human kidney. *Proc Natl Acad Sci U S A* 91: 6943–6947, 1994
25. Uchida S, Sasaki S, Furukawa T, Hiraoka M, Imai T, Hirata Y, Marumo F: Molecular cloning of a chloride channel that is regulated by dehydration and expressed predominantly in kidney medulla. *J Biol Chem* 268: 3821–3824, 1993
26. Trotti D, Peng JB, Dunlop J, Hediger MA: Inhibition of the glutamate transporter EAAC1 expressed in *Xenopus* oocytes by phorbol esters. *Brain Res* 914: 196–203, 2001
27. Fahlke Ch, Knittle TJ, Gurnett CA, Campbell KP, George AL Jr: Subunit stoichiometry of human muscle chloride channels. *J Gen Physiol* 109: 93–104, 1997
28. Jurman ME, Boland LM, Liu Y, Yellen G: Visual identification of individual transfected cells for electrophysiology using antibody-coated beads. *Biotechniques* 17: 876–881, 1994
29. Hebeisen S, Biela A, Giese B, Muller-Newen G, Hidalgo P, Fahlke Ch: The role of the carboxyl terminus in ClC chloride channel function. *J Biol Chem* 279: 13140–13147, 2004
30. Cheng C, Glover G, Banker G, Amara SG: A novel sorting motif in the glutamate transporter excitatory amino acid transporter 3 directs its targeting in Madin-Darby canine kidney cells and hippocampal neurons. *J Neurosci* 22: 10643–10652, 2002
31. Daniels GM, Amara SG: Selective labeling of neurotransmitter transporters at the cell surface. *Methods Enzymol* 296: 307–318, 1998